Mitigating the Impact of Increased Drought-Flood Abrupt Alternation Events under Climate Change: The Role of Reservoirs in the Lancang-Mekong River Basin

Keer Zhang[1], Zilong Zhao[1], Fuqiang Tian[1,2]

[1]Department of Hydraulic Engineering & State Key Laboratory of Hydroscience and Engineering, Tsinghua University, 100084, Beijing, China

[2]Southwest United Graduate School, Kunming 650091, China

Correspondence to: Fuqiang Tian (tianfq@mail.tsinghua.edu.cn)

Abstract. The Lancang-Mekong River (LMR) Basin is highly vulnerable to extreme hydrological events, including Drought-Flood Abrupt Alternation (DFAA). The impact of climate change on DFAA and the efficacy of potential mitigation measures such as reservoirs remain poorly understood. This study investigates these dynamics using five Global Climate Models (GCMs) from the Coupled Model Intercomparison Project Phase 6 (CMIP6). It employs the Revised Short-cycle Drought-Flood Abrupt Alteration Index (R-SDFAI), alongside the Tsinghua Representative Elementary Watershed (THREW) model integrated with the developed reservoir module. Results reveal that future DFAA trend varies widely in upstream and downstream, with significant increases respectively in FTD (flood to drought) upstream and DTF (drought to flood) downstream. FTD is more challenging though DTF is more probable to occur. Under low- and medium-emission scenarios, DFAA risks escalate, especially during the wet season, whereas under high-emission scenario, their risks decline. Reservoirs as a promising adaptation strategy can significantly mitigate the year-round DTF and wet season's FTD, particularly in regions with higher total reservoir storage. Reservoir operations reduce DFAA's risks, limit multiple peaks and shorten its monthly span. Hydrological forecasting and resilient storage are viable options for climate change to help LMR Basin smooth out DFAA. These insights offer valuable guidance for effective water resources cooperative management across LMR Basin countries.

Keywords. Drought-Flood Abrupt Alternation; Climate change; Reservoir operation; Lancang-Mekong River Basin.

1. Introduction

Flood and drought are the two most frequent natural disasters in the world (Adikari et al., 2009;

ADREM et al., 2024). Drought-Flood Abrupt Alternation (DFAA), defined as the rapid transition flood and drought (Xiong et al., 2025), has received growing attention in recent years (Chen et al., 2025; Wu et al., 2023; Zhang et al., 2012; Shan et al., 2018; Song et al., 2023). DFAA is specifically divided into the rapid change from flood to drought (FTD) and from drought to flood (DTF). Hazards arising from DFAA are more significant compared to floods and droughts. DFAA not only alters the soil condition and increases the potential for exceeding water quality standard (Bai et al., 2023; Yang et al., 2019), but also challenges food security and seriously affects agricultural production. Furthermore, DFAA, particularly DTF is exposed to triggering severe secondary natural hazards, primarily including flash floods, landslides, and mudslides (Wang et al., 2023).

Employing indices to characterize DFAA events is a common quantitative method. Since Wu et al. (2006) proposed the precipitation-based long-cycle drought-flood abrupt alternation index (LDFAI) to quantitatively characterize the long-term DFAA of wet season, LDFAI has been widely adopted (Ren et al., 2023; Shi et al., 2021; Yang et al., 2022; Yang et al., 2019). Zhang et al. (2012) proposed the one-month interval short-cycle drought-flood abrupt alternation index (SDFAI) based on LDFAI to characterize the short-term DFAA of wet season, and expanded the application from precipitation to runoff. SDFAI has been extensively applied in various fields such as hydrology, meteorology, ecology, and agriculture (Zhao et al., 2022; Lei et al., 2022; Yang et al., 2019; Zhang et al., 2019). Song et al. (2023) further refined the SDFAI index and developed the Revised Short-cycle Drought-Flood Abrupt Alteration Index (R-SDFAI), which is calculated based on the Standardized Runoff Index (SRI) and designed to characterize short-term DFAA.

It has been observed that the intensity and frequency of DFAA events demonstrate a global increasing trend (Yang et al., 2022; Chen et al., 2024). However, regional differences are notable. Shan et al. (2018) observed that the scope of DFAA events in the Yangtze River mid-lower reaches has expanded since the 1960s, with both frequency and intensity increasing annually. Zhang et al. (2012) found that while droughts and floods in the Huai River Basin have increased, DFAA events have become less frequent. For future projections, Zhao et al. (2022) indicated that DFAA events in the Han River Basin will experience an upward trend in both frequency and intensity. Yang et al. (2019) reported that in the Hetao region, the number and frequency of DFAA events will diminish.

Lancang-Mekong River (LMR) Basin, as an important international river in Southeast Asia, profoundly affects Southeast Asia's important industries such as hydropower, agriculture, fisheries and transport

(Morovati et al., 2024), while also being the high incidence area of floods and droughts (Liu et al., 2020; MRC, 2020). It is reported that wet season's drought accounts for about 40% of annual drought (Tian et al., 2020) and there is the potential for large floods to happen in the dry season (e.g., May 2006, May 2007, and December 2016) (Tellman et al., 2021). These non-negligible wet season's drought and dry season's flood are all prerequisites for DFAA.

Continued global warming will further exacerbate extreme wet and dry climate (IPCC, 2023) and contribute to the increased vulnerability of DFAA in future (Yang et al., 2022; Wang et al., 2023; Chen et al., 2025). There is a strong tendency for floods and droughts to intensity in Southeast Asia (IPCC WG1, 2021) as well as in LMR Basin (Wang et al., 2021; Li et al., 2021; Dong et al., 2022; Hoang et al., 2016). This warns of the serious DFAA pattern in LMR Basin and puts forward new requirements for water security and sustainable management, especially the early disaster forecasting and prevention system.

The hydrological regime of LMR Basin is influenced by two main drivers, climate change and human activities (LMC and MRC, 2023). Despite the severity of climate change impacts, human activity is capable of adapting to climate change in the hydrological regime in LMR Basin (Zhang et al., 2023; Khadka et al., 2023; Sridhar et al., 2019; Lu et al., 2014; Gunawardana et al., 2021), such as reservoir operation. Research has shown that reservoirs play a crucial role in preventing extensive damages during the wet season and in minimizing low-flow occurrences in LMR Basin (Arias et al., 2014; Räsänen et al., 2012; Dang et al., 2024). The integration of a coupled reservoir module within the hydrological model is a widely adopted approach for evaluating reservoir impacts under changing climate. Wang et al. (2017b) utilized this approach to show that reservoir operation can minimize flood intensity and lower flood occurrence rates. Yun et al. (2021a; 2021b) demonstrated that, despite a trade-off in hydroelectric benefits, reservoir management can substantially alleviate extreme drought and wet hydrological events in LMR Basin. These studies collectively indicated that reservoirs represent a practical solution for addressing the impacts of climate change.

It is crucial to consider the adaptation role of human activities, represented by reservoirs, to DFAA under climate change, which helps managers to develop effective policies on water resources management and ensures sustainable development of the basin system. However, little attention has been paid to this aspect for LMR Basin in previous studies. The statistic, report, and study related to DFAA in LMR Basin are almost empty currently, let alone the impact of climate change and the mitigating role of reservoirs on DFAA. Therefore, this study develops the reservoir module for hydrological modelling, highlights the trend of DFAA in LMR Basin under climate change, and explores how reservoirs assist basin states to adapt changing climate. It endeavors to generate new knowledge into DFAA and contributes to water resource management and regional sustainability.

2. Methodology

2.1 Study area

The Lancang-Mekong River (LMR) originates from the Tibetan Plateau in China and flows through China, Myanmar, Laos, Thailand, Cambodia, and Vietnam before entering the South China Sea at the Mekong Delta. LMR is approximately 4900 km long, with the basin area of 812400 km^2 (He, 1995), and its annual runoff is approximately 475 billion m^3 (Sabo et al., 2017; Luo et al., 2023). LMR Basin is characterized by steep slopes and rapid flows in the upstream, along with shallow slopes and slow mixed flows in the downstream. The wet and dry seasons in LMR Basin extend from June to November and from December to May (LMC and MRC, 2023), which are mainly influenced by southwestern and northeastern monsoons respectively. The distribution of the hydrology system and mainstream hydrological stations in LMR Basin are detailed in Fig. 1a.

LMR Basin nourishes approximately 65 million people. The basin states rely on the river system to develop economic industries including capture fisheries, irrigation agriculture, and hydropower. LMR Basin has the largest freshwater capture fishery in the world (MRC, 2010; MRC, 2019), and its irrigation area is estimated around 4.3 million hectares (Do et al., 2020), with the Mekong Delta regarded as Southeast Asia's food basket. LMR Basin is one of the most active regions for hydropower in the world (MRC, 2019; Williams, 2019), harboring about 235,000 $GWh \cdot yr^{-1}$ of hydroelectric potential in its mainstream and tributaries (Do et al., 2020; Schmitt et al., 2018). LMR Basin meanwhile is heavily impacted by flood and drought. During past two decades, LMR Basin has experienced several severe droughts (2004-2005, 2009-2010, 2015-2016, and 2019-2020) and floods (Liu et al., 2020; Tian et al., 2020; MRC, 2020), which affects crop cultivation and fisheries harvesting, causing loss of property and lives in riparian countries. Floods of 2013 and 2018 heavily affected the lower basin (Cambodia, Vietnam, Laos, and Thailand), covering 22.3 and 6.47 thousand km^2 respectively (Tellman et al., 2021).

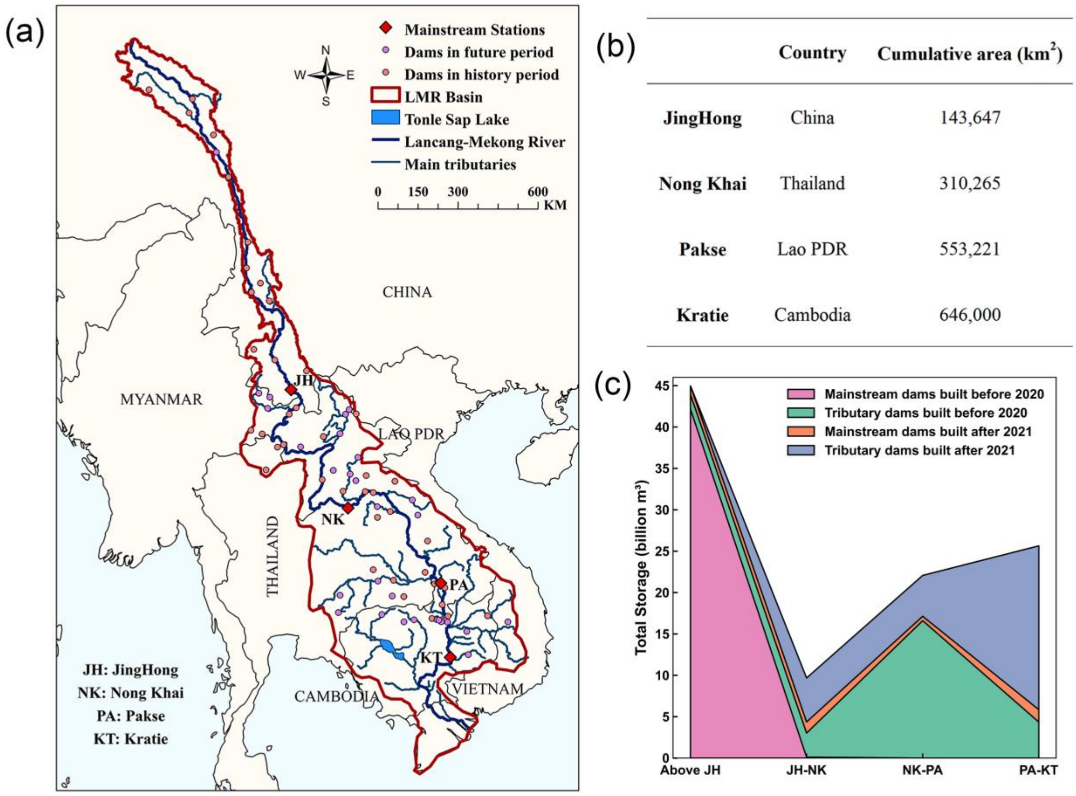

Figure 1: Hydrology of LMR Basin. (a) Map of rivers and reservoirs, (b) Information of four main hydrological stations, and (c) distribution of reservoir storage. Here, JH, NK, PA, and KT respectively denote JingHong, Nong Khai, Pakse, and Kratie stations.

2.2 Data collection

This study utilizes CMIP6 (Sixth Phase of Coupled Model Inter-comparison Project) data as the meteorological input to analyze DFAA. Three SSP (Shared Socioeconomic Pathways) scenarios, namely SSP1-2.6, SSP2-4.5, and SSP5-8.5, are considered to characterize the low-, medium-, and high-emission scenarios respectively. Five GCMs (Global Climate Models) with wide utilization and proven performance in LMR Basin are applied in this study (Li et al. 2021; Yun et al., 2021a; Yun et al., 2021b), i.e., GFDL-ESM4, IPSL-CM6A-LR, MPI-ESM1-2-HR, MRI-ESM2-0, and UKESM1-0-LL. The detailed information for these five GCMs is shown in Table 1 (Eyring et al., 2016; Gidden et al., 2019; Cui et al., 2023). CMIP6 data span from 1980 to 2100. This study accordingly considers three research periods, namely history period from 1980 to 2014 (consistent with CMIP6), near future period from 2021 to 2060, and far future period from 2061 to 2100.

In this study, the daily observed runoff data at four major mainstream hydrological stations from 1980 to 2020 serve to calibrate and validate the hydrological model, and these data are derived from China Meteorological Administration (CMA) and Mekong River Commission (MRC). The hydrological stations from upstream to downstream are sequentially JingHong, Nong Khai, Pakse and Kratie, whose locations and basic information are shown in Figs. 1a and 1b. This study treats the ERA5_Land data as the meteorological input when calibrating and validating the hydrological model, and as the correction dataset when correcting the raw CMIP6 data. ERA5_Land data cover the period from 1980 to 2020, with the spatial resolution of 0.1°, and contain precipitation, temperature, and potential evapotranspiration. Soil data are obtained from the Global Soil Database (GSD) provided by the Food and Agriculture Organization of the United Nations (FAO) with the spatial resolution of 10 x 10 km. Normalized Vegetation Index (NDVI), Leaf Area Index (LAI) and Snow Cover data are obtained from MODIS (Moderate-resolution Imaging Spectroradiometer) with a spatial resolution of 500 x 500 m and a temporal resolution of 16 days.

Reservoir data are sourced from MRC and Mekong Region Futures Institute (MERFI) (MERFI, 2024). 122 reservoirs which simultaneously contain information on location, storage and operation years are utilized in this study, including 24 reservoirs in Lancang Basin and 98 reservoirs in Mekong Basin. The earliest and latest operation years for them are 1965 and 2035. The location and storage distribution of these reservoirs are shown in Figs. 1a and 1c.

Model Name	Modeling Center	Realization	Resolution (Lon×Lat)
GFDL-ESM4	National Oceanic and Atmospheric Administration Geophysical Fluid Dynamics Laboratory, United States	r1i1p1f1	1.25°×1°
IPSL-CM6A-LR	Institute Pierre Simon Laplace, France	r1i1p1f1	2.5°×1.25874°
MPI-ESM1-2-HR	Max Planck Institute for Meteorology, Germany	r1i1p1f1	0.9375°×0.9375°
MRI-ESM2-0	Meteorological Research Institute, Japan	r1i1p1f1	1. 125°×1. 125°
UKESM1-0-LL	Met Office Hadley Centre, UK	r1i1p1f2	1.875°×1.25°

Table 1: Details of 5 GCMs applied in this study.

2.3 Bias correction method for CMIP6 data

The raw CMIP6 data require correction for more accurate modelling (Hoang et al., 2016; Mishra et al., 2020; Sun et al., 2023). The uncorrected raw CMIP6 data misestimate the temperature and precipitation in LMR Basin, especially overestimating the precipitation (Cui et al., 2023; Lange et al., 2019; Lange et al., 2021). ERA5_Land data are applied as the correction data in this study to correct bias in raw CMIP6 data.

This study interpolates the five GCMs data of CMIP6 with different spatial resolutions to 0.1° (consistent with ERA5_Land) based on the bilinear interpolation spatial resolution method. The interpolated CMIP6 data are bias-corrected for each GCM according to N-dimensional probability density function transform of the multivariate bias correction approach (abbreviated as MBCn) (Cannon, 2016; Cannon, 2018). The MBCn method is trained based on the difference between precipitation and temperature data from ERA5_Land and CMIP6 over history period (1980-2014), and then applied to future period (i.e., 2021-2100) to correct the CMIP6 data for each GCM.

The MBCn method considers the multivariate dependency structure of meteorological data and enables the simultaneous correction of temperature and precipitation data. Random orthogonal rotation and quantile delta mapping are the two most critical formulas of the MBCn method (Cannon, 2018), as illustrated in Eqs. (1) and (2).

$$\begin{cases} \tilde{\boldsymbol{X}}_T^{[j]} = \boldsymbol{X}_T^{[j]}\boldsymbol{R}^{[j]} \\ \tilde{\boldsymbol{X}}_S^{[j]} = \boldsymbol{X}_S^{[j]}\boldsymbol{R}^{[j]} \\ \tilde{\boldsymbol{X}}_P^{[j]} = \boldsymbol{X}_P^{[j]}\boldsymbol{R}^{[j]} \end{cases} \tag{1}$$

Eq. (1) displays the process of random orthogonal rotation. It outlines the process of transforming historical observations $X_T^{[j]}$, historical climate model simulations $X_S^{[j]}$, and climate model projections $X_P^{[j]}$ using a random orthogonal rotation matrix $R^{[j]}$ during the j-th iteration. The rotated data are represented as $\tilde{X}_T^{[j]}$, $\tilde{X}_S^{[j]}$, and $\tilde{X}_P^{[j]}$. This procedure is pivotal for MBCn's multivariate joint distribution correction, as it transforms the original variable space into new random orientations. In contrast to conventional uni-variate correction approaches, MBCn employs a random orthogonal matrix to mix variables, thereby breaking their independence.

$$\begin{cases} \Delta^{(n)[j]}(i) = \tilde{x}_P^{(n)[j]}(i) - F_S^{(n)[j]^{-1}}\left(F_P^{(n)[j]}\left(\tilde{x}_P^{(n)[j]}(i)\right)\right) \\ \hat{x}_P^{(n)[j]}(i) = F_T^{(n)[j]^{-1}}\left(F_P^{(n)[j]}\left(\tilde{x}_P^{(n)[j]}(i)\right)\right) + \Delta^{(n)[j]}(i) \end{cases} \tag{2}$$

Eq. (2) exhibits the quantile delta mapping, which defines how quantile delta mapping is applied to n-th dimension of the rotated climate model projection data $\tilde{x}_P^{(n)[j]}(i)$ within the rotated space of the j-th iteration. Here, $\Delta^{(n)[j]}(i)$ represents the quantile difference between the historical climate model simulations and climate model projections in the j-th iteration and the n-th dimension. $F_P^{(n)[j]}$ denotes the empirical cumulative distribution function for the rotated climate model projection data in the n-th dimension. $F_T^{(n)[j]^{-1}}$ and $F_S^{(n)[j]^{-1}}$ denote inverse Functions of the empirical cumulative distribution functions for the rotated historical observation data and historical climate model simulation data in the n-th dimension. This step preserves the trend of the climate model projection data throughout the correction process. The number of iterations is typically set to 10-30.

The MBCn algorithm performs multivariate joint distribution bias correction by iteratively applying the random orthogonal rotation and quantile delta mapping, while preserving the projected signals in the climate model. The rotation operation breaks dependencies between variables, enabling the quantile delta mapping of single variable to indirectly adjust multivariate correlations. The quantile delta mapping ensures the transmission of absolute or relative trends by computing quantile differences between the historical and projected periods of the climate model. The MBCn method demonstrates a significant improvement in terms of correction precision and accuracy, compared to uni-variate bias correction algorithms along with other multivariate bias correction algorithms (Cannon, 2018).

In addition, this study utilized the method proposed by Van Pelt et al. (2009) to compute daily potential evapotranspiration data for five GCMs under three SSP scenarios, based on daily air temperature. The computational approach is outlined in Eq. (3).

$$\mathrm{PET} = [1 + \alpha_0(\mathrm{T} - \overline{\mathrm{T}_0})]\overline{\mathrm{PET}_0} \tag{3}$$

Where, $\overline{\mathrm{T}_0}$ and $\overline{\mathrm{PET}_0}$ correspond to the daily air temperature (°C) and daily potential evapotranspiration (mm day^{-1}) in the history period sourced from ERA5_Land datasets. T signifies the corrected daily air temperature (°C) from CMIP6 datasets. The parameter α_0 is determined by the relationship between daily potential evapotranspiration and daily temperature in ERA5_Land data during the history period.

2.4 Hydrological model coupled with reservoir module

The THREW (Tsinghua Representative Elementary Watershed) hydrological model is applied in this study for runoff simulation. It utilizes the Representative Elementary Watershed (REW) approach for spatial division, and further subdivides the REW into eight distinct hydrological zones: vegetated zone, bare soil zone, glacier covered zone, snow covered zone, sub-stream-network zone, main channel reach, saturated zone, and unsaturated zone (Tian et al., 2006; Mou et al., 2008).

The model is built upon scale coordinated equilibrium equations, geometrical relationships and constitutive relationships, and enables to comprehensively simulate complex hydrological processes from mountain to ocean. The fundamental balance equations in the THREW model are listed in Eqs. (4) to (6).

$$\frac{d}{dt}(\overline{\rho^j_\alpha}\epsilon^j_\alpha y^j \omega^j) = \sum_P e^{jP}_\alpha + \sum_{\beta\neq\alpha} e^j_{\alpha\beta} \tag{4}$$

Eq. (4) demonstrates the general form of mass conservation equation at the REW scale. $\frac{\mathrm{d}}{\mathrm{dt}}$ denotes the time derivative. $\overline{\rho_\alpha^j}$ refers to the time-averaged density of phase α in sub-region j, in $\mathrm{kg \cdot m^{-3}}$. ϵ_α^j means the volume fraction of phase α within sub-region j. $\mathrm{y^j}$ indicates the time-averaged thickness of sub-region j, in m. ω^j means the time-averaged fraction of REW horizontal area occupied by sub-region j. e_α^{jP} denotes the net mass exchange flux of phase α in sub-region j through interface P (e.g., with atmosphere, groundwater, neighboring REWs), in $\mathrm{kg \cdot m^{-2} \cdot s^{-1}}$, with the positive value indicating the inflow to sub-region j. $\mathrm{e}_{\alpha\beta}^j$ refers to the phase transition rate between phase α and phase β within sub-region j, in $\mathrm{kg \cdot m^{-2} \cdot s^{-1}}$, with the positive value meaning phase α gains mass from phase β. Sub-region here refer to the divided eight zones within each REW.

$$(\overline{\rho_\alpha^j}\epsilon_\alpha^j y^j \omega^j)\frac{d\overline{v_\alpha^j}}{dt} = \overline{g_\alpha^j \rho_\alpha^j}\epsilon_\alpha^j y^j \omega^j + \sum_P T_\alpha^{jP} + \sum_{\beta \neq \alpha} T_{\alpha\beta}^j \quad (5)$$

Eq. (5) presents the general form of momentum conservation equation at the REW scale. $\overline{\mathrm{v}_\alpha^j}$ indicates the time-averaged velocity vector of phase α in sub-region j, in $\mathrm{m \cdot s^{-1}}$. $\overline{\mathrm{g}_\alpha^j}$ denotes the time-averaged gravity vector of phase α in sub-region j, in $\mathrm{m \cdot s^{-2}}$. T_α^{jP} means the force vector (pressure, friction, seepage) exerted on phase α in sub-region j by interface P, in $\mathrm{N \cdot s^{-2}}$, representing the momentum exchange. $\mathrm{T}_{\alpha\beta}^j$ refers to the interfacial force vector between phase α and phase β within sub-region j, in $\mathrm{N \cdot s^{-2}}$, including drag and capillarity.

$$(\epsilon_\alpha^j y^j \omega^j c_\alpha^j)\frac{d\overline{\theta_\alpha^j}}{dt} = \overline{h_\alpha^j \rho_\alpha^j}\epsilon_\alpha^j y^j \omega^j + \sum_P Q_\alpha^{jP} + \sum_{\beta \neq \alpha} Q_{\alpha\beta}^j \quad (6)$$

Eq. (6) exhibits the general form of heat conservation equation at the REW scale. c_α^j means the specific heat capacity (constant volume) of phase α in sub-region j, in $\mathrm{J \cdot kg^{-1} \cdot K^{-1}}$. θ_α^j refers to the time-averaged temperature of phase α in sub-region j, in K. $\overline{h_\alpha^j}$ denotes the heat generation rate per unit mass within phase α in sub-region j, in $\mathrm{W \cdot kg^{-1}}$ (e.g., radioactive decay, negligible usually). Q_α^{jP} indicates the heat exchange rate between phase α in sub-region j and its environment via interface P, in $\mathrm{W \cdot m^{-2}}$, with the positive value representing the heat is gained by phase α in sub-basin j. $\mathrm{Q}_{\alpha\beta}^j$ refers to the heat exchange rate between phase α and phase β within sub-region j, in $\mathrm{W \cdot m^{-2}}$, with the positive value indicating the heat is gained by phase α.

The THREW model employs an automatic calibration procedure to calibrate hydrological parameters through parallel computation (Nan et al., 2021). The calibration period of THREW model in LMR Basin is from 2000 to 2009, and the validation period is from 2010 to 2020. The Nash-Sutcliffe efficiency coefficient (NSE) indicator is adopted to calibrate the objective function and evaluate simulation effectiveness at daily scale, which is calculated according to Eq. (7). THREW model has been successfully applied to a number of basins with various climate characteristics worldwide (Tian et al., 2012; Lu et al., 2021; Morovati et al., 2023; Cui et al., 2023; Zhang et al., 2023).

$$\mathrm{NSE} = 1 - \frac{\sum_{n=1}^{N}(Q_o^n - Q_s^n)^2}{\sum_{n=1}^{N}(Q_o^n - \overline{Q_o})^2} \tag{7}$$

Where, Q_o^n is the daily observed runoff, Q_s^n is the daily simulated runoff, $\overline{Q_o}$ is the average of observed runoff, and N is the total number of days.

This study extends the THREW model through the development of a reservoir management module that can be incorporated into it. This module contains detailed data on 122 reservoirs in the basin, with operational years ranging from 1965 to 2035. Configuring the module's activation enables the integrated THREW model to simulate natural runoff without considering reservoirs, and dammed runoff with reservoirs considered.

The reservoir operation rules are consistent over time and space, with each reservoir following the same operation rules and starting scheduling according to its respective operational year. The reservoir module conducts daily-scale reservoir operation based on sub-basins. Each reservoir is allocated to the corresponding sub-basin according to its location information. The cumulative reservoir storage over multiple years for each sub-basin is calculated and serves as an input condition for the reservoir module. The module consists of two phases: the initial phase and the normal phase. The constraints of the normal phase are further divided into general and emergency cases. Both cases share the same reservoir operation rules, but their constraints differ, with the emergency case featuring more flexible constraints. The reservoir module's flowchart is depicted in Fig. 2.

When the cumulative multi-year storage of some REW changes in one year, it indicates that at least one new reservoir starts operation in that REW in that year. The additional reservoir operates under the initial phase rules. The rules for initial phase are described as Eqs. (8) to (9). The outlet flow is equal to the inlet flow if the inlet flow is less than the minimum discharge constraint, and otherwise equal to the minimum discharge constraint. Constraints on storage and discharge are summarized in Eqs. (10) to (11) (Tennant, 1976; Yun et al., 2020). The ending condition for the initial phase is Eq. (12). When the storage of the additional reservoir is larger than the minimum storage constraint, end the initial phase and enter the normal phase.

$$Q_{out} = \begin{cases} Q_{in}, Q_{in} < Q_{min} \\ Q_{min}, Q_{in} \geq Q_{min} \end{cases} \tag{8}$$

$$S_t = S_{t-1} + Q_{in} - Q_{out} \tag{9}$$

$$S_{min} = 0.2 \times S_{total} \tag{10}$$

$$Q_{min} = 0.6 \times Q_{ave} \tag{11}$$

$$S_t \geq S_{min} \tag{12}$$

Where Q_{out} is the outlet flow, Q_{in} is the inlet flow, Q_{min} is the minimum discharge constraint, S_t is the storage for time t, S_{min} is the minimum storage constraint, S_{total} is the total storage, and Q_{ave} is the average multi-year runoff during calibration period (i.e., 2000-2009).

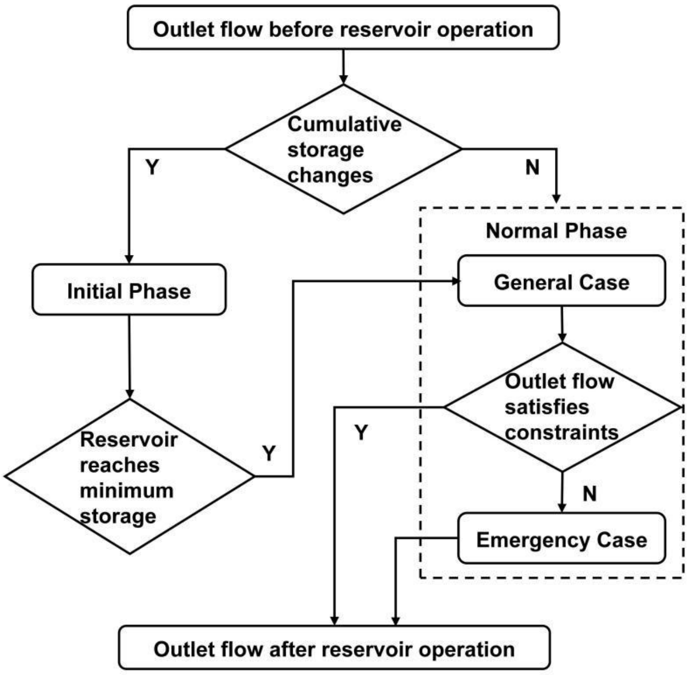

Figure 2: Flowchart of the constructed reservoir module.

The scheduling rule for the normal phase is the improved Standard Operation Policy hedging model (SOP) (Wang et al., 2017a; Morris & Fan, 1998), as depicted in Eq. (9) and Eqs. (13) to (16). Under the premise of water balance (Eq. (9)), constraints for annual storage (Eq. (13)), outlet flow (Eq. (14)), wet season storage (Eq. (15)), and dry season storage (Eq. (16)) are considered separately, where priority is given to the annual storage constraint (Eq. (13)).

$$S_{min} \leq S_t \leq S_{max} \tag{13}$$

$$Q_{min} \leq Q_{out} \leq Q_{max} \quad (14)$$

$$\min|S_c - S_t|, \text{month} = 6,7,8,9,10,11 \quad (15)$$

$$\min|S_n - S_t|, \text{month} = 12,1,2,3,4,5 \quad (16)$$

Where Q_{max} is the maximum discharge constraint, S_{max} is the maximum storage constraint, S_c is the storage corresponding to the flood control level, and S_n is the storage corresponding to the normal storage level.

When the reservoir enters the normal phase, constraints of the general case are used by default. Constraints for the general case are given in Eqs. (17) to (22). After scheduling according to general case's constraints, if the outlet flow constraint is not fully satisfied (Eq. (14)), constraints are adjusted to that in the emergency case and the reservoir is re-operated following adjusted constraints. Eq. (23) characterizes the start condition for the emergency case. The emergency case is set to avoid excessive high or low outlet flow caused by the strict constraints. Constraints of the emergency case are shown in Eqs. (24) to (25).

$$Q_{max} = 2 \times Q_{ave} \quad (17)$$

$$Q_{min} = 0.6 \times Q_{ave} \quad (18)$$

$$S_c = S_{min} \times 1.2 \quad (19)$$

$$S_n = S_{max} \times 0.8 \quad (20)$$

$$S_{min} = 0.2 \times S_{total} \quad (21)$$

$$S_{max} = \begin{cases} 0.8 \times S_{total}, \text{month} = 6,7,8,9,10,11 \\ 1 \times S_{total}, \text{month} = 12,1,2,3,4,5 \end{cases} \quad (22)$$

$$Q_{min} \leq Q_{out}' \leq Q_{max} \quad (23)$$

$$Q_{min} = 0.3 \times Q_{ave} \quad (24)$$

$$S_{max} = 0.8 \times S_{total} \quad (25)$$

Where Q_{out}' is the outlet flow after the scheduling in general case.

2.5 Indicator for DFAA

The Revised Short-cycle Drought-Flood Abrupt Alteration Index (R-SDFAI), as put forward by Song et al. (2023), extends the applicable time frame from the flood season of LDFAI and SDFAI to cover the entire year, making it more suitable for multi-year DFAA analysis. Furthermore, it successfully mitigates issues like over-identification, under-identification, and inaccurate representation of DFAA severity inherent in SDFAI. Thus, this study adopts R-SDFAI for DFAA analysis. The formulas for R-SDFAI are summarized in Eqs. (26) to (31) (Song et al., 2023).

$$F_1 = S_{i+1} - S_i \tag{26}$$

$$F_2 = |S_{i+1}| + |S_i| \tag{27}$$

$$F = \left|\frac{F_1}{F_2}\right|^{|S_{i+1}+S_i|} \tag{28}$$

$$I = F \times \min(|S_{i+1}|, |S_i|) \tag{29}$$

$$I' = \left(\frac{I}{0.5}\right)^{\frac{\max(|S_{i+1}|,|S_i|)^2}{|F_1|+F_2}} \times \frac{I^{\frac{\max(|S_{i+1}|,|S_i|)}{|F_1|+F_2}} + I^{\frac{\min(|S_{i+1}|,|S_i|)}{|F_1|+F_2}}}{2} \tag{30}$$

$$R - SDFAI = \mathrm{sign}(F_1) \times \left(\frac{I'}{I'_{0.5}} \times \frac{I}{0.5}\right)^{\left[\frac{\max(|S_{i+1}|,|S_i|)}{|F_1|+F_2}\right]^{\left[1-\frac{\max(|S_{i+1}|,|S_i|)}{|F_1|+F_2}\right]}} \tag{31}$$

Where, S_i refers to the SRI in month i, F1 denotes the intensity of DFAA, F2 denotes the absolute intensity of drought and flood, and F is a weighting factor between 0 and 1. $I'_{0.5}$ refers to I' when I=0.5.

The calculation process of SRI utilized in this work is explained in Eqs. (32) to (37). Eq. (32) gives the probability density function that satisfies the Gamma distribution for runoff x at a given time period.

$$g(x) = \frac{1}{\beta^{\alpha}\Gamma(\alpha)} x^{\alpha-1} e^{-\frac{x}{\beta}}, \quad x > 0 \tag{32}$$

where, $\alpha > 0$ and $\beta > 0$ are respectively the shape and scale parameters. $\widehat{\alpha}$ and $\widehat{\beta}$ are the optimal values of α and β, obtained according to the maximum likelihood estimation method, as illustrated in Eqs. (33) to (35). $\Gamma(\alpha)$ is the gamma function, as given in Eq. (36).

$$\widehat{\alpha} = \frac{1}{4A}\left(1 + \sqrt{1 + \frac{4A}{3}}\right. \tag{33}$$

$$\widehat{\beta} = \frac{\bar{x}}{\widehat{\alpha}} \tag{34}$$

$$A = \ln(\bar{x}) - \frac{\sum \ln(x_i)}{n} \tag{35}$$

$$\Gamma(\alpha) = \int_0^{\infty} y^{\alpha-1} e^{y}\, dy \tag{36}$$

Where, x_i is the sample of runoff sequence, $\bar{x}$ is averaged runoff, and n is the length of runoff sequence.

Then the cumulative probability of runoff x is illustrated in Eq. (37).

$$G(x) = \int_0^{x} g(x)\, dx = \frac{1}{\hat{\beta}^{\hat{\alpha}}\Gamma(\hat{\alpha})} \int_0^{x} x^{\hat{\alpha}-1} e^{-\frac{x}{\hat{\beta}}} dx, \quad x > 0 \tag{37}$$

The threshold for R-SDFAI to recognize DFAA events is ± 1, which indicates that the identified DFAA event is at least an abrupt transition between a mild hydrological drought event ($SRI < -1$) and a mild hydrological wet event ($SRI > 1$) (Song et al., 2023). When R-SDFAI > 1, DTF occurs, and when R-SDFAI < -1, FTD occurs.

2.6 Scenario Setting

This study concentrates on two scenarios: dammed and natural scenarios. The meteorological data from five selected GCMs under three SSPs are downscaled from grid scale to REW scale and served as meteorological inputs for the THREW model. The THREW model, augmented with the reservoir module, is applied to simulate runoff at key mainstream hydrological stations during history (1980-2014), near future (2021-2060), and far future (2061-2100) periods, examining both scenarios with and without reservoir management. The R-SDFAI indicator is then employed to assess the probabilities of DFAA events for each study period within both dammed and natural scenarios, utilizing the runoff data generated by the 5 GCMs and 3 SSPs.

This study adopts the difference in DFAA's probability between natural (without reservoir operations) and dammed scenarios (considering reservoir operations) to capture reservoir's impact, as shown in Eq. (38).

$$P_{\text{Impact of Reservoirs},i,t} = P_{\text{Dammed},i,t} - P_{\text{Natural},i,t} \tag{38}$$

Where $P_{\text{Impact of Reservoirs},i,t}$ represents the impact of reservoirs on the probability of event t in period i. $P_{\text{Natural},i,t}$ denotes the probability of event t under the natural scenario in period i while the $P_{\text{Dammed},i,t}$ denotes the probability of event t under the dammed scenario in period i. Period i refers to the near future period and the far future period. Event t indicates the DTF events, FTD events and DFAA events. Eqs. (39) and (40) gives the definitions of $P_{\text{Natural},i,t}$ and $P_{\text{Dammed},i,t}$ described above.

$$P_{Natural,i,t} = \frac{M_{Natura,i,t}}{TM_i} \tag{39}$$

$$P_{Dammed,i,t} = \frac{M_{Dammed,i,t}}{TM_i} \tag{40}$$

Where $M_{Natura,i,t}$ denotes the number of months in which event t occurs in period i under the natural scenario. $M_{Dammed,i,t}$ denotes the number of months occurred event t occurs in period i under the dammed scenario. TM_i refers to the total number of months in period i. Period i refers to the near future period and the far future period. Event t indicates the DTF events, FTD events and DFAA events. As each GCM possesses unique structure and assumptions, projections of climate change by a single GCM inherently possess uncertainties, which in turn introduce uncertainties in the simulation of hydrological outcomes (Kingston et al., 2011; Thompson et al., 2014). Thus, averaging across multiple GCMs is a crucial approach, as it minimizes model biases, eliminates outliers, reduces uncertainties, and ensures more robust and universally applicable outcomes (Lauri et al., 2012; Hoang et al., 2016; Hecht et al., 2019; Wang et al., 2024; Yun et al., 2021b). This method has been extensively employed in prior studies (Dong et al., 2022; Li et al., 2021; Wang et al., 2022; Yun et al., 2021a). Therefore, this research determines the average DFAA probability from five GCMs to lessen the uncertainty in their predictions and assesses the fluctuation in these probabilities across the models to demonstrate their variability.

3. Result

3.1 CMIP6 data bias correction performance

From both regional and seasonal perspectives, the uncorrected raw CMIP6 data exhibits significant discrepancies with ERA5_Land data during history period (1980-2014). When compared with ERA5_Land data for history period, the uncorrected raw CMIP6 data reveals an average annual precipitation bias of ±1800 mm and an average daily temperature of ±12℃ (Figs. 3b and 3e). These notable inconsistencies underscore that hydrological modeling using uncorrected raw CMIP6 data would incur considerable inaccuracies. However, CMIP6 data corrected by MBCn method deviate from ERA5_Land data within ±120 mm of average annual precipitation and ±0.2℃ of average daily temperature (Figs. 3c and 3f). The bias correction significantly improves the accuracy of CMIP6 data in LMR Basin. Meanwhile, the corrected CMIP6 data match the seasonal cycle of ERA5_Land well in both precipitation and temperature (Fig. 3g). With respect to raw CMIP6 data before correction, the spatial and temporal distribution accuracy of corrected CMIP6 improves dramatically, which contributes to more accurate and reasonable analyses for DFAA.

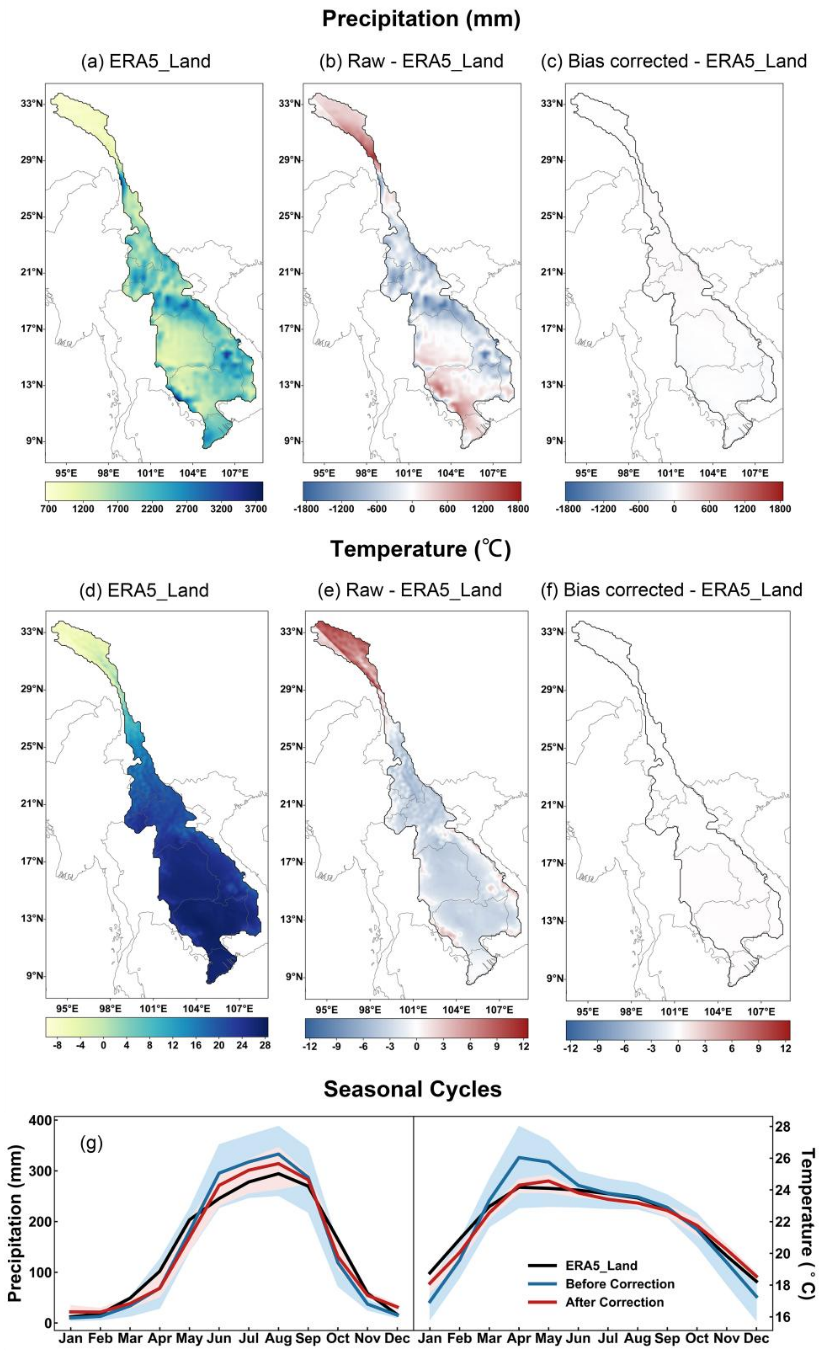

Figure 3: Averaged meteorological data of 5 GCMs for history period (1980-2014). Here, 5 GCMs are corrected separately. (a)-(c) present the spatial distribution of precipitation based on respectively ERA5_Land, raw CMIP6 (raw CMIP6 minus ERA5_Land) and bias-corrected CMIP6 (bias-corrected CMIP6 minus ERA5_Land). (d)-(f) illustrate the spatial distribution of temperature based on ERA5_Land, raw CMIP6 (raw CMIP6 minus ERA5_Land) and bias-corrected CMIP6 (bias-corrected CMIP6 minus ERA5_Land). (g) seasonal cycles of temperature and precipitation from ERA5_Land, raw and bias-corrected CMIP6, as well as their corresponding range.

3.2 Calibration and validation for hydrological model

The daily observed runoff versus daily simulated runoff given by THREW model for calibration period (2000-2009) and validation period (2010-2020) are illustrated in Fig. 4. Since there was no massive reservoir construction in LMR Basin before and during calibration period (Zhang et al., 2023), THREW model without reservoir module is applied for calibration period. Meanwhile, part of large scale reservoirs have been commissioned during validation period, thus THREW model configuration with reservoir module is validated in validation period. THREW model captures the runoff fluctuation between wet and dry seasons well, with an NSE of at least 0.8 during calibration and validation periods. THREW model exhibits excellent simulation performance in both upstream and downstream regions.

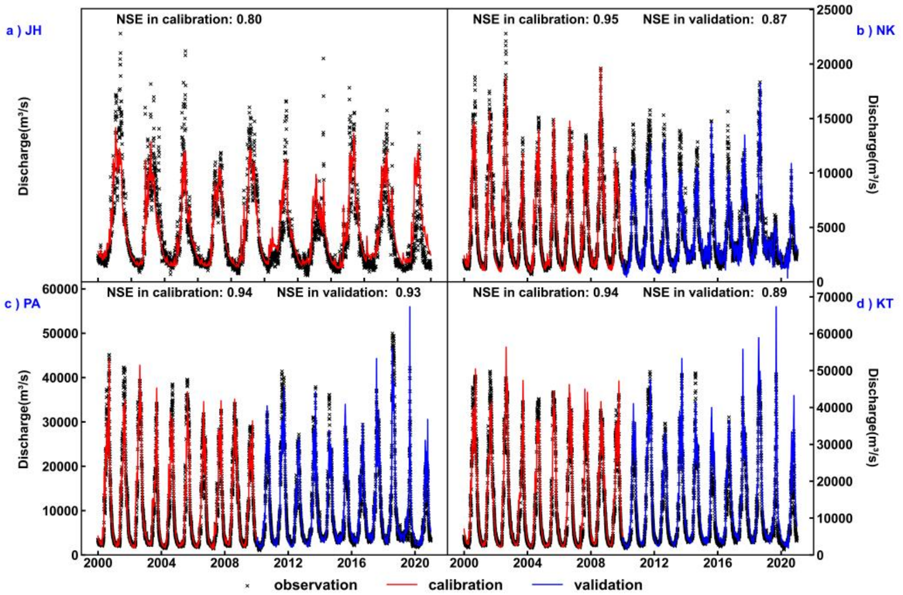

Figure 4: Performance of THREW model in calibration (2000-2009) and validation (2010-2020) periods. Here, JH, NK, PA, and KT denote JingHong, Nong Khai, Pakse, and Kratie stations, respectively.

3.3 DFAA under changing climate

Under natural scenario (without reservoir operations), DFAA in LMR Basin is dominated by DTF, i.e., the risk of DTF is more critical than that of FTD. DFAA risk moreover is significantly higher in the wet season than dry season (Fig. 5a). For the average of five GCMs, the probability of FTD in the wet season is 2 to 5.5 times higher than that in the dry season in history period. In the near and far future periods, this ratio respectively ranges from 1.1 to 36 times and 3.3 to 41 times. As for DTF, the probability in the wet season is correspondingly 1.7 to 5.7 times, 1.3 to 3.9 times and 0.9 to 6.3 times higher than that in the dry season for history, near future and far future. Only JingHong station experiences a slightly higher probability of DTF in the dry season (1.25%) than in the wet season (1.17%) for far future. Furthermore, the annual probability in DFAA is higher remarkably downstream than upstream (Fig. 5a). The annual FTD's probability ranges from 1.1% to 2.5% at JingHong station and 1.3% to 2.8% at Nong Khai station. These probabilities rises to 2.3% to 4.2% and 2.7% to 4.1% at Pakse and Kratie stations. Similarly, the annual DTF's probability at JingHong and Nong Khai stations are 2.4% to 4.1% and 2.3% to 4.5%. These probabilities at Pakse and Kratie stations reaches 3.7% to 6.3% and 4.2% to 6.3%. The DTF risk in the wet season and FTD risk in both dry and wet seasons are also higher downstream than upstream. Since the FTD probability in the dry season at Nong Khai, Pakse and Kratie stations is limited, especially under SSP5-8.5 scenario (<0.2%), the FTD risk of dry season appears more notable at upstream than downstream.

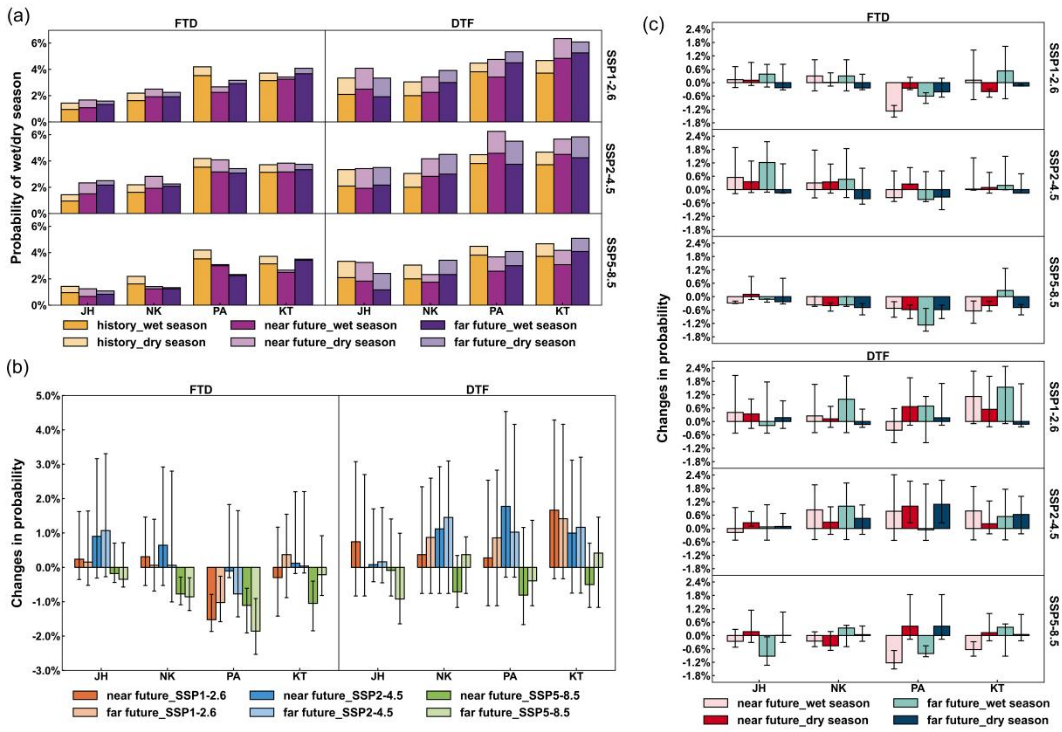

Figure 5: DFAA under natural scenario. Here, JH, NK, PA, and KT respectively denote JingHong, Nong Khai, Pakse, and Kratie stations. (a) Seasonal probability of DFAA averaged across five GCMs during history (1980-2014), near future (2021-2060) and far future (2061-2100) periods, as well as under three SSPs. The annual probability is half of the sum of wet and dry season probabilities. (b) The annual change in DFAA probability averaged across five GCMs and their ranges in the near and far future periods with respect to history period under three SSPs. (c) The seasonal change in DFAA probability averaged across five GCMs and their ranges in the near and far future periods with respect to history period during wet and dry seasons under three SSPs.

The annual DFAA risk increases under SSP1-2.6 and SSP2-4.5 scenarios (except for FTD at Pakse station) and decreases under SSP5-8.5 scenario (Fig. 5b). Among three scenarios, SSP5-8.5 is characterized by the lowest DFAA risk. Under this scenario, the average probability of FTD across five GCMs is 1.1% to 3.5%, while the DTF probability ranges from 2.3% to 5.1%. Conversely, SSP2-4.5 is associated with the highest DFAA risk, with FTD and DTF probabilities respectively averaging 1.4% to 4.1% and 3.4% to 6.3%. Further, the future growth in DTF is significantly greater than that of FTD. For the average probabilities across five GCMs, relative to the history period, the future change in DTF probability at JingHong station is -0.4% to 1.1%, at Nong Khai station is -0.9% to -0.6%, and at Pakse and Kratie stations respectively is -1.9% to -0.1% and -1% to 0.4%. The future FTD probability change for JingHong is -0.9% to 0.2%, while it is -0.7% to 1.5%, -0.8% to 1.8%, and -0.5% to 1.7% for Nong Khai, Pakse and Kratie, respectively. The maximum values from the five GCMs show consistent trends, with DTF probability increases being significantly greater than FTD probability increases. Additionally, upstream regions face more significant increases in FTD risks in the future, while downstream regions experience a more substantial rise in DTF risks. The opposite trends of DFAA risk in upstream and downstream pose enhanced challenges to the integrated management of LMR Basin. The DFAA risk, meanwhile, increases most significantly under SSP2-4.5 scenario, while under SSP5-8.5 FTD risk drops and the growth of DTF risk is also negligible. Similar to the annual DFAA risk, the wet-season risks for both DTF and FTD rise under SSP1-2.6 and SSP2-4.5 scenarios, and fall under SSP5-8.5 scenario (Fig. 5c). The FTD risk of dry season is reduced, with an increase observed only under SSP2-4.5 in the near future (average across five GCMs <0.4%, maximum <1.3%). The dry-season risk for DTF rises in all situations, except at Nong Khai station under SSP5-8.5 in the near future, where it shows an average decrease of 0.46% across five GCMs. The largest increase is observed at Pakse station under SSP2-4.5, with an average increase of 1.08% across five GCMs and a maximum increase of 2.08%.

3.4 Reservoirs' impacts on DFAA

Reservoirs exhibit extraordinary mitigation effects on DTF risk under changing climate while showing weaker effects in FTD risk. (Fig. 6a). Nonetheless, the higher probability of DTF compared to FTD (Fig. 5a) demonstrates that reservoirs contribute significantly to reducing overall DFAA risk. Reservoirs adequately reduce or only slightly increase the future DTF probability (-0.13% to 1%, averaged across five GCMs), and in most scenarios, the reservoir plays a positive mitigating role across all GCMs (Fig. 6a). Reservoirs exhibit better mitigation effects in the near future at JingHong station. As for Nong Khai and Pakse stations, The reduction effect of reservoirs on DTF is more pronounced in the far future under SSP1-2.6 and SSP2-4.5 scenarios while in the near future under SSP5-8.5 scenario. The effect conversely exhibits greater strength under SSP1-2.6 and SSP5-8.5 scenarios in the near future while it is stronger under SSP2-4.5 scenario in the far future at Kratie station. These findings are consistent across both the average of the GCMs and their ranges.

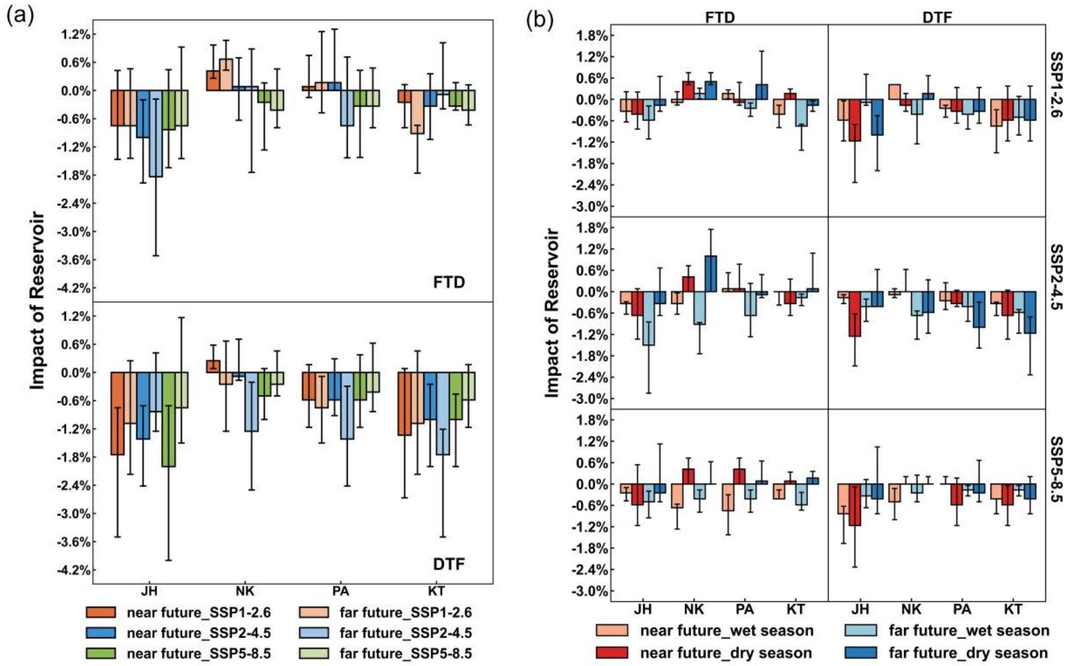

Figure 6: Reservoir impacts on DFAA during near future (2021-2060) and far future (2061-2100) under three SSPs. Here, JH, NK, PA, and KT denote JingHong, Nong Khai, Pakse, and Kratie stations, respectively. (a) The annual reservoir impacts averaged across five GCMs and their ranges. (b) The seasonal reservoir impacts in wet and dry seasons averaged across five GCMs and their ranges.

The reduction effect of reservoirs on FTD performs slightly better in the near future (0.42%, averaged across five GCMs) than far future (0.38%, averaged across GCMs) at JingHong station, while slightly greater in the far future (both 0.21%, GCM average) than in the near future (0.13% and 0.17%, GCM average) at Nong Khai and Kratie stations, while it remains the same in the near and far future periods at Pakse station (both 0.17%, GCM average). Reservoirs show the best effects under the SSP5-8.5 scenario, in which they effectively alleviate the FTD probability at all hydrological stations (0.13% to 0.42%, GCM average). Under SSP1-2.6 and SSP2-4.5 scenarios, although the reservoir operation displays poor mitigation effects (-0.33% to 0.38%, GCM average) at Nong Khai and Pakse stations, it demonstrates notable mitigating effects at JingHong and Kratie stations, particularly in certain scenarios. For instance, under SSP2-4.5 scenario of the far future at JingHong station, the reservoir reduces the average probability across GCMs by over 1.8% and lowers the maximum probability values by nearly 3.6%.

Furthermore, reservoirs exhibit superior mitigation capacity against DFAA at JingHong and Kratie compared to Nong Khai and Pakse stations, which aligns with the storage distribution in LMR Basin (Fig. 1c). Both the average and maximum probability values across five GCMs confirm this pattern. This indicates that reservoirs not only function well in flood and drought control (Hecht et al., 2019; Hoang et al., 2019; Ly et al., 2023), but respond excellently to unexpected events such as DFAA.

The reduction effect of reservoirs on FTD in the wet season (-0.17% to 1.5%, averaged across GCMs) appears to be more remarkable compared to that in the dry season (-1% to 0.67%, GCM average), especially at Nong Khai, Pakse and Kratie stations (Fig. 6b). Reservoirs generally demonstrate significant reduction effects on FTD in the wet season (-0.17% to 0.92%, GCM average) at these stations, however, increase FTD probability in the dry season (-1% to 0.33%, GCM average). Seasonal differences of reservoirs mitigation effects on DTF are not as significant as those for FTD. Reservoirs achieve slightly better reduction effects in the dry season (-0.17% to 1.25%, GCM average) on DTF than in the wet season (-0.42% to 0.83%, GCM average). Moreover, the reservoir displays superior mitigation capability in DTF relative to FTD in both dry and wet seasons, which is consistent with the annual DFAA.

DFAA tends to exhibit multiple monthly peaks under natural scenario, implying there are multiple months with higher DFAA probability than their adjacent months. The multiple peaks are more pronounced in DTF than FTD (Fig. 7). As for the monthly DFAA averaged over four mainstream hydrological stations, DTF shows triple peaks under near-term SSP2-4.5 scenario and far-term SSP5-8.5 scenario, while FTD both exhibits double peaks. The reservoir serves to regulate DFAA by reducing peaks and decreasing the number of peaks, where its reduction effect on the number of peaks appears more pronounced in the near future and for DTF (Fig. 7). Reservoirs provide robust peak alleviation for far future and FTD, particularly under SSP1-2.6 and SSP2-4.5 scenarios, despite their limited contribution in decreasing the number of peaks. Reservoirs meanwhile remarkably reduce DFAA probability in early and middle dry season (i.e., December to April) for both near and far future, lowering it to within 1% or even 0% (averaged across five GCMs) for most stations. The reservoir furthermore potently shortens DFAA's monthly span from spread out the whole year for natural scenario to concentrated from May to October for dammed scenario (Fig. 7), which enables LMR Basin to centralize relevant policies and practices on DFAA to this period. It therefore facilitates riparian states to integrate resources and concentrate efforts on targeted water resources management to achieve enhanced response to and control of DFAA along with its secondary hazards.

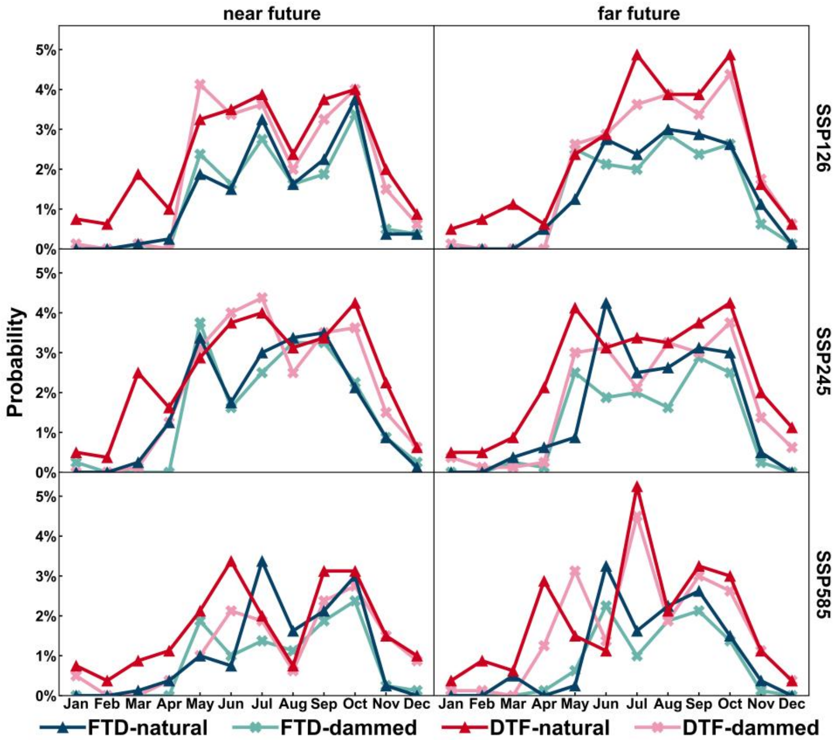

Figure 7: Monthly DFAA probability averaged over four mainstream hydrological stations (i.e., JingHong, Nong Khai, Pakse and Kratie stations) under natural and dammed scenarios for three SSPs during near future (2021-2060) and far future (2061-2100) periods. Please note that the probabilities shown in this figure are averaged over 5 GCMs.

4. Discussion

4.1 Different characteristics of DTF and FTD under changing climate

Although flood and drought risks in LMR Basin will decrease respectively in the near and far future periods (Li et al., 2021; Hoang et al.,2016; Wang et al., 2017b; Yun et al., 2021a; Yun et al., 2021b), DFAA risk will still increases under SSP1-2.6 and SSP2-4.5 scenarios (Fig. 5). DTF and FTD exhibit quite different characteristics, in that DTF is more frequent but FTD is more challenging.

The distinct characteristics of DTF and FTD events have been identified by previous research. Shi et al. (2021) found that FTD events are predominant in the Wei River Basin. Wang et al. (2023) projected that in the Poyang Lake Basin, the temporal spread of DTF events will expand in future, while that of FTD events will constrict. Ren et al. (2023) found that under SSP1-2.6 and SSP2-4.5 scenarios, the Huang-Huai-Hai River Basin will experience more DTF events, but under SSP3-7.0 and SSP5-8.5 scenarios, it will experience more FTD events.

The probability of DTF is significantly higher than FTD (Fig. 5a) and rises considerably in the near and far future periods (Fig. 5b). However, reservoirs well control the DTF probability and significantly reduce the DTF risk in both dry and wet seasons (Fig. 6). This can be attributed to the fact that the DTF's demand for water regulation follows the reservoir scheduling logic, whereby the reservoir releases water to alleviate drought during early DTF, when reservoirs stay at low water level, which exactly satisfies the storage requirements of the sudden flood in late DTF.

Comparatively, although FTD is less probable than DTF, reservoirs poorly control it, especially in the dry season, which is pertinent to the challenge that reservoirs hardly spare capacity for floods in early FTD whilst ensuring storage for drought during late FTD. FTD tends to occur unexpectedly under the high incidence of DTF, and the current reservoir operation struggles to perfectly control its risk, which leads to extreme challenges in FTD. Fortunately, the probability of FTD however will drop in most areas of LMR Basin in future (Fig. 5).

4.2 Reservoir operation integrated with hydrological forecast

Future DFAA in LMR Basin remains severe (Fig. 5). Although reservoirs provide positive impacts to DFAA under changing climate, there is room for improvement in some situations (Fig. 6). This is attributed to the fact that relying on general reservoir operation rules such as SOP alone can't fully realize reservoirs' potential (Zhang et al., 2018), and these rules are scheduled with completely unknown incoming flows. The reservoir's ability in responding to DFAA will be further enhanced if being scheduled with known incoming flows. Reservoir scheduling combined with hydrological forecast is a practical approach.

Hydrological forecasting technology enhances the potential of reservoirs, improves their ability to address disasters and optimizes the resilience of LMR Basin system. Hydrological forecast enables the prediction of reservoirs inflows and extreme hydrological events at appropriate time scales according to actual requirements (Brunner et al., 2021b; Ibrahim et al., 2022), and assists in assessing their severity and possible impacts on production and livelihoods in LMR Basin (Kao et al., 2020; Kumar et al., 2023;

Prodhan et al., 2022; Hao et al., 2018).

Hydrological forecasts provide insights into runoff and disaster situations, enabling the adaptation of reservoirs' current and future operational procedures. This adjustment can maximize reservoirs' water management efficiency, effectively counteracting flood-induced drought (FTD) and drought-induced flood (DTF). For instance, when a flood is occurring and hydrological forecasts predict an impending drought, reservoirs' operational methods should be modified to both reserve adequate storage capacity for the next flood event and maximize water retention to counteract the subsequent drought. Likewise, if hydrological forecasts indicate that a flood will strike after the current drought, reservoir management will transition from maximizing water storage to ensuring water availability during the drought while also setting aside adequate storage capacity for the upcoming flood event. In necessary situations, especially when severe disasters are forecasted, it is advisable to consider sacrificing some of the hydroelectric benefits, making the maintenance of normal production and living in LMR Basin the primary objective of reservoir operation.

4.3 Maximizing utilization of the resilient storage

The mitigation effect of reservoirs on DFAA risk is closely associated with the storage distribution of mainstream and tributary reservoirs (Figs. 1c and 6). This finding emphasizes a strong connection between reservoir storage capacity and its mitigation potential on DFAA. It aligns with Ehsani et al. (2017), who suggested that expanding dam dimensions can offset the vulnerability of water resources to climate uncertainties, and Feng et al. (2024), whose study highlighted the effectiveness of large reservoirs in mitigating drought and flood risks.

This study exclusively examines hydroelectric reservoirs in LMR Basin, excluding other water storage facilities like irrigation reservoirs and minor irrigation systems. The LMR Basin, however, boasts significant storage capacity through these additional facilities. The MRC reports 1317 irrigation reservoirs in Mekong Basin, with total storage about 17 billion m³ (MRC, 2018; LMC and MRC, 2023). This storage surpasses than of reservoirs between JingHong and Nong Khai stations (around 9.7 billion m³), and is marginally less than those between Nong Khai to Pakse region stations (approximately 22.1 billion m³), as depicted in Fig. 1c.

The existing research has pointed out that the mitigating effect of reservoirs on extreme hydrological events is independent of their main purpose. Even when their main purpose isn't directly tied to mitigating such events, they can still offer significant benefits (Brunner, 2021a; Ho et al., 2025). This study thus emphasizes the need for rationally planning and use of irrigation reservoirs in LMR Basin, particularly during severe DFAA situations. By integrating these reservoirs as adjustable storage solutions alongside hydroelectric reservoirs, the basin's ability to handle DFAA can be enhanced, thereby boosting the system's resilience and adaptability.

5. Conclusion

This study adopts CMIP6 meteorological data under three SSP scenarios and five GCMs, and corrects them utilizing MBCn method. Combined hydrological model THREW and the developed reservoir module, it applies R-SDFAI to characterize DFAA, and explores the mitigating role of reservoirs on DFAA under changing climate in LMR Basin. The study periods are organized into history (1980-2014), near future (2021-2060) and far future (2061-2100). The main findings are summarized below:

1. Future DFAA trend varies widely in upstream and downstream of LMR Basin, with significant rises in upstream FTD and downstream DTF. While DTF occurs more probable, FTD presents more challenge. Annual and wet-season risks of DFAA increase under SSP1-2.6 and SSP2-4.5 scenarios. The DFAA risk is considerably higher in the wet season than dry season.
2. Reservoirs competently reduce year-round risk of DTF and wet season's risk of FTD in LMR Basin, and perform better in regions with larger total storage of mainstream and tributary reservoirs. Moreover, reservoirs contribute markedly to control DFAA's multiple peaks and to shorten its monthly span.
3. Hydrological forecast and resilient storage are able to help smoothly survive DFAA, and could be robust options to address climate change.

This study provides new insights into the mitigating role of reservoirs on DFAA in LMR Basin and contributes to water resources management for riparian countries. DFAA remains severe under climate change and reservoirs do contribute to mitigating it, thus this study calls for information sharing and joint actions among basin countries on the forecast and prevention of DFAA. The joint efforts of LMR Basin states will facilitate exploring more effective and feasible measures to mitigate impacts of climate change and facilitate the long-term sustainable development.

Author contribution

KZ: Conceptualization; Data curation; Model development; Investigation; Methodology; Validation; Visualization; Writing - original draft; Writing - review & editing. **ZZ**: Writing - review & editing. **FT:** Conceptualization; Funding acquisition; Investigation; Methodology; Supervision; Writing - review & editing.

Competing interests

At least one of the (co-)authors is a member of the editorial board of Hydrology and Earth System Sciences.

Data availability

The hydrological data can be accessed and requested from the MRC Data Portal (https://portal.mrcmekong.org/home, last access: March 2025). Information related to dams is available on the Mekong Region Futures Institute (MERFI) website (https://www.merfi.org/mekong-region-dams-database, last access: March 2025). The raw CMIP6 data without correction is available at (https://esgf-node.llnl.gov/search/cmip6/, last access: March 2025). The MBCn algorithm can be accessed and implemented through an R package, which is available at (https://CRAN.R-project.org/package=MBC, last access: July, 2025).

Acknowledgment

This research was funded by the National Natural Science Foundation of China (51961125204, U2442201).

Reference

Adikari, Y., Yoshitani, J.: Global Trends in Water-Related Disasters: An Insight for Policymakers, International Centre for Water Hazard and Risk Management (ICHARM). The United Nations World Water Development Report 3, Tsukuba, Japan, https://unesdoc.unesco.org/ark:/48223/pf0000181793 (last access: March 2025), 2009.

ADREM, SNSE, NDRC, IFRC and IRDR: 2023 Global Natural Disaster Assessment Report. Bejing, https://reliefweb.int/report/world/2023-global-natural-disaster-assessment-report (last access: March 2025), 2024.

Arias, M.E., Piman, T., Lauri, H., Cochrane, T.A., Kummu, M.: Dams on Mekong tributaries as significant contributors of hydrological alterations to the Tonle Sap Floodplain in Cambodia. Hydrol.

Earth Syst. Sci. 18, 5305-5315. https://doi.org/10.5194/hess-18-5303-2014, 2014.

Bai X., Zhao C., Tang Y., Zhang Z., Yang B. and Wang Z.: Identification, physical mechanisms and impacts of drought–flood abrupt alternation: a review. Front. Earth Sci. 11:1203603, https://doi.org/10.3389/feart.2023.1203603, 2023.

Brunner, M.: Reservoir regulation affects droughts and floods at local and regional scales. Environ. Res. Lett. 16 (12). https://doi.org/10.1088/1748-9326/ac36f6, 2021a.

Brunner, M. I., Slater, L., Tallaksen, L. M., Clark, M.: Challenges in modeling and predicting floods and droughts: A review. WIREs Water, 8(3), e1520, https://doi.org/10.1002/wat2.1520, 2021b.

Chen Z., Li X., Zhang X., et al.: Global drought-flood abrupt alternation: Spatio-temporal patterns, drivers, and projections. The Innovation Geoscience 3:100113, https://doi.org/10.59717/j.xinn-geo.2024.100113, 2025.

Cui, T., Li, Y., Yang, L., Nan, Y., Li, K., Tudaji, M., Tian, F.: Non-monotonic changes in Asian Water Towers' streamflow at increasing warming levels. Nature Communication, 14(1), 1176, https://doi.org/10.1038/s41467-023-36804-6, 2023.

Cannon, A. J.: Multivariate Bias Correction of Climate Model Output: Matching Marginal Distributions and Intervariable Dependence Structure. J. Clim. 29, 7045–7064, https://doi.org/10.1175/JCLI-D-15-0679.1, 2016

Cannon, A. J.: Multivariate quantile mapping bias correction: an N-dimensional probability density function transform for climate model simulations of multiple variables. Clim. Dyn. 50, 31–49, https://doi.org/10.1007/s00382-017-3580-6, 2018.

Dang, H. and Pokhrel, Y.: Evolution of river regimes in the Mekong River basin over 8 decades and the role of dams in recent hydrological extremes, Hydrol. Earth Syst. Sci., 28, 3347–3365, https://doi.org/10.5194/hess-28-3347-2024, 2024.

Do, P., Tian, F., Zhu, T., Zohidov, B., Ni, G., Lu, H., Liu, H.: Exploring synergies in the water-food-energy nexus by using an integrated hydro-economic optimization model for the Lancang-Mekong River basin. Sci. Total Environ. 728, 137996, https://doi.org/10.1016/j.scitotenv.2020.137996, 2020.

Dong, Z., Liu, H., Baiyinbaoligao, Hu, H., Khan, M., Wen, J., Chen, L., Tian, F.: Future projection of seasonal drought characteristics using CMIP6 in the Lancang-Mekong River Basin. J. Hydrol. 610, https://doi.org/10.1016/j.jhydrol.2022.127815, 2022.

Ehsani, N., Vörösmarty, C., Fekete, B., Stakhiv, E.: Reservoir operations under climate change: storage capacity options to mitigate risk. J. Hydrol. 555, 435–446. https://doi.org/10.1016/j.jhydrol.2017.09.008, 2017.

Eyring, V., Bony, S., Meehl, G. A., Senior, C. A., Stevens, B., Stouffer, R. J., and Taylor, K. E.: Overview of the Coupled Model Intercomparison Project Phase 6 (CMIP6) experimental design and organization, Geosci. Model Dev., 9, 1937–1958, https://doi.org/10.5194/gmd-9-1937-2016, 2016.

Feng, J., Qin, T., Yan, D., Lv, X., Yan, D., Zhang, X., Li, W.: The role of large reservoirs in drought and flood disaster risk mitigation: a case of the Yellow River Basin. Sci. Total Environ. 949, 175255. https://doi.org/10.1016/j.scitotenv.2024.175255, 2024.

Gidden, M. J., Riahi, K., Smith, S. J., Fujimori, S., Luderer, G., Kriegler, E., van Vuuren, D. P., van den Berg, M., Feng, L., Klein, D., Calvin, K., Doelman, J. C., Frank, S., Fricko, O., Harmsen, M., Hasegawa, T., Havlik, P., Hilaire, J., Hoesly, R., Horing, J., Popp, A., Stehfest, E., and Takahashi, K.: Global emissions pathways under different socioeconomic scenarios for use in CMIP6: a dataset of harmonized emissions trajectories through the end of the century, Geosci. Model Dev., 12, 1443–1475, https://doi.org/10.5194/gmd-12-1443-2019, 2019.

Gunawardana, S.K., Shrestha, S., Mohanasundaram, S., Salin, K.R., Piman, T.: Multiple drivers of hydrological alteration in the transboundary Srepok River Basin of the Lower Mekong Region. J. Environ. Manage. 278, 111524, https://doi.org/10.1016/j.jenvman.2020.111524, 2021.

Hao, Z., Singh, V. P., Xia, Y.: Seasonal drought prediction: Advances, challenges, and future prospects. Reviews of Geophysics, 56, 108–141, https://doi.org/10.1002/2016RG000549, 2018.

He D.: Analysis on the hydrological characteristics of Lancang-Meigong River. Yunnan Geographic Environment Research, 1, 58-74 (in Chinese), 1995.

Hecht, J.S., Lacombe, G., Arias, M.E., Dang, T.D., Piman, T.: Hydropower dams of the Mekong River basin: A review of their hydrological impacts. J. Hydrol. 568, 285–300, https://doi.org/10.1016/j.jhydrol.2018.10.045, 2019.

Ho, S. Q.-G. and Ehret, U.: Is drought protection possible without compromising flood protection? Estimating the potential dual-use benefit of small flood reservoirs in southern Germany, Hydrol. Earth Syst. Sci., 29, 2785–2810, https://doi.org/10.5194/hess-29-2785-2025, 2025.

Hoang, L. P., Lauri, H., Kummu, M., Koponen, J., van Vliet, M. T. H., Supit, I., Leemans, R., Kabat, P., and Ludwig, F.: Mekong River flow and hydrological extremes under climate change, Hydrol. Earth Syst. Sci., 20, 3027–3041, https://doi.org/10.5194/hess-20-3027-2016, 2016.

Hoang, L.P., van Vliet, M.T.H., Kummu, M., Lauri, H., Koponen, J., Supit, I., Leemans, R., Kabat, P., Ludwig, F.: The Mekong's future flows under multiple drivers: How climate change, hydropower developments and irrigation expansions drive hydrological changes. Sci. Tot. Environ, https://doi.org/10.1016/j.scitotenv.2018.08.160, 2019.

Ibrahim, K.S.M.H., Huang, Y.F., Ahmed, A.N., Koo, C.H., El-Shafie, A.: A review of the hybrid artificial intelligence and optimization modelling of hydrological streamflow forecasting. Alex. Eng. J. 61 (1), 279–303, https://doi.org/10.1016/j.aej.2021.04.100, 2022.

IPCC: Sections. In: Climate Change 2023: Synthesis Report. Contribution of Working Groups I, II and III to the Sixth Assessment Report of the Intergovernmental Panel on Climate Change [Core Writing Team, H. Lee and J. Romero (eds.)]. IPCC, Geneva, Switzerland, pp. 35-115, https://doi.org/10.59327/IPCC/AR6-9789291691647, 2023.

IPCC Working Group I contribution to the Sixth Assessment Report of the Intergovernmental Panel on Climate Change. Climate Change; The Physical Science Basis. TS-93, https://www.ipcc.ch/report/ar6/syr/ (last access: March 2025), 2021.

Kao, I.F., Zhou, Y., Chang, L.C., Chang, F.J.: Exploring a long short-term memory based encoder-decoder framework for multi-step-ahead flood forecasting. Journal of Hydrology 124631, https://doi.org/10.1016/j.jhydrol.2020.124631, 2020.

Khadka, D., Babel, M. S., Kamalamma, A. G.: Assessing the Impact of Climate and Land-Use Changes on the Hydrologic Cycle Using the SWAT Model in the Mun River Basin in Northeast Thailand. Water, 15, 3672, https://doi.org/10.3390/w15203672, 2023.

Kingston, D. G., Thompson, J. R., and Kite, G.: Uncertainty in climate change projections of discharge for the Mekong River Basin, Hydrol. Earth Syst. Sci., 15, 1459–1471, https://doi.org/10.5194/hess-15-1459-2011, 2011.

Kumar, V., Azamathulla, H. M., Sharma, K. V., Mehta, D. J., Maharaj, K. T.: The State of the Art in Deep Learning Applications, Challenges, and Future Prospects: A Comprehensive Review of Flood Forecasting and Management. Sustainability, 15(13), 10543, https://doi.org/10.3390/su151310543, 2023.

Lancang-Mekong Water Resources Cooperation Center (LMC) and Mekong River Commission (MRC): Technical Report - Phase 1 of the Joint Study on the Changing Patterns of Hydrological Conditions of the Lancang-Mekong River Basin and Adaptation Strategies. Beijing: LMC Water Center or Vientiane: MRC Secretariat, http://www.lmcwater.org.cn/cooperative_achievements/collaborative_projects/ (last access: March 2025), https://www.mrcmekong.org/publication/ (last access: March 2025), 2023.

Lange, S.: Trend-preserving bias adjustment and statistical downscaling with ISIMIP3BASD (v1.0), Geoscientific Model Development, 12, 3055–3070, https://doi.org/10.5194/gmd-12-3055-2019, 2019.

Lange, S.: ISIMIP3BASD v2.5.0, https://doi.org/10.5281/zenodo.4686991, 2021.

Lauri, H., de Moel, H., Ward, P. J., Räsänen, T. A., Keskinen, M., and Kummu, M.: Future changes in Mekong River hydrology: impact of climate change and reservoir operation on discharge, Hydrol. Earth Syst. Sci., 16, 4603–4619, https://doi.org/10.5194/hess-16-4603-2012, 2012.

Lei X., Song X., Guo H., Ma R., Song S.: Analysis on spatio-temporal evolution characteristics of short-cycle drought-flood sudden alteration and potential driving factors in the north-south transitional zone of China. Journal of Natural Disasters. 31(4), 31-43 (in Chinese), https://doi.org/10.13577/j.jnd.2022.0403, 2022.

Li, Y., Lu, H., Yang, K., Wang, W., Tang, Q., Khem, S., Yang, F., Huang, Y.: Meteorological and hydrological droughts in Mekong River Basin and surrounding areas under climate change, J. Hydrol.: Reg. Stud. 36, 100873, https://doi.org/10.1016/j.ejrh.2021.100873, 2021.

Liu, H., Yang, Z., Xu, F., Zhang, X., Baiyin, B., Mu, X., Hu, H.: Drought in Lancang-Mekong River Basin and the impact of upstream reservoirs. J. China Inst. Water Resour. Hydropower Res. 6, 479–485 (in Chinese), https://doi.org/10.13244/j.cnki.jiwhr.20200058, 2020.

Lu, Y., Tian, F., Guo, L., Borzì, I., Patil, R., Wei, J., Liu, D., Wei, Y., Yu, D. J., Sivapalan, M.: Socio-hydrologic modeling of the dynamics of cooperation in the transboundary Lancang–Mekong River, Hydrol. Earth Syst. Sci., 25, 1883–1903, https://doi.org/10.5194/hess-25-1883-2021, 2021.

Lu, X.X., Li, S., Kummu, M., Padawangi, R., Wang, J. J.: Observed changes in the water flow at Chiang Saen in the lower Mekong: impacts of Chinese dams? Quatern. Int., https://doi.org/10.1016/j.quaint.2014.02.006, 2014.

Luo, X., Luo, X., Ji, X., Ming, W., Wang, L., Xiao, X., Xu, J., Liu, Y., Li, Y.: Meteorological and hydrological droughts in the Lancang-Mekong River Basin: spatiotemporal patterns and propagation. Atmospheric Research 293, 106913. https://doi.org/10.1016/j.atmosres.2023.106913, 2023.

Ly, S., Sayama, T., Try, S.: Integrated impact assessment of climate change and hydropower operation on streamflow and inundation in the lower Mekong Basin. Prog Earth Planet Sci 10, 55, https://doi.org/10.1186/s40645-023-00586-8, 2023.

MERFI: Dataset on the Dams of the Greater Mekong. Bangkok, Mekong Region Futures Institute, https://www.merfi.org/mekong-region-dams-database (last access: March 2025), 2024.

Mishra, V., Bhatia, U., Tiwari, A.D.: Bias-corrected climate projections for South Asia from Coupled Model Intercomparison Project-6. Sci Data 7, 338, https://doi.org/10.1038/s41597-020-00681-1, 2020.

Morovati, K., Tian, F., Kummu, M., Shi, L., Tudaji, M., Nakhaei, P., Olivares, M. A.: Contributions from climate variation and human activities to flow regime change of Tonle Sap Lake from 2001 to 2020. Journal of Hydrology, 616, 128800, https://doi.org/10.1016/j.jhydrol.2022.128800, 2023.

Morovati, K., Tian, F., Pokhrel, Y., Someth, P., Shi, L., Zhang, K., Ly, S.: Fishery and agriculture amidst human activities and climate change in the Mekong River: A review of gaps in data and effective approaches towards sustainable development, J. Hydrol., 132043, https://doi.org/10.1016/j.jhydrol.2024.132043, 2024.

Morris, G. L., & Fan, J.: Reservoir sedimentation handbook: Design and management of dams, reservoirs, and watersheds for sustainable use. New York, NY: McGraw-Hill, 1998.

Mou, L., Tian, F., Hu, H., and Sivapalan, M.: Extension of the Representative Elementary Watershed approach for cold regions: constitutive relationships and an application, Hydrol. Earth Syst. Sci., 12, 565–585, https://doi.org/10.5194/hess-12-565-2008, 2008.

MRC: Assessment of Basin-Wide Development Scenarios—Main Report, Mekong River Commission, https://reliefweb.int/report/lao-peoples-democratic-republic/assessment-basin-wide-development-scenarios-main-report (last access: March 2025), 2010.

MRC: Irrigation Database Improvement for the Lower Mekong Basin. Vientiane, Lao PDR, https://www.mrcmekong.org/publications/irrigation-database-improvement-for-the-lower-mekong-river-basin/#:~:text=It%20reviews%20the%20current%20situation%20of%20irrigation%20in,%28LMB%29%20and%20provides%20recommendations%20for%20further%20database%20impro (last access: March 2025), 2018.

MRC: State of the Basin Report 2018, https://www.mrcmekong.org/publications/state-of-the-basin-report-2018-2/ (last access: March 2025), 2019.

MRC: Annual Mekong hydrology, flood and drought report 2019: Drought in the Lower Mekong River Basin. Vientiane: MRC Secretariat, https://www.mrcmekong.org/publications/annual-mekong-hydrology-flood-and-drought-report-2019-drought-in-the-lower-mekong-basin/ (last access: March 2025), 2020.

Nan, Y., Tian, L., He, Z., Tian, F., and Shao, L.: The value of water isotope data on improving process understanding in a glacierized catchment on the Tibetan Plateau, Hydrol. Earth Syst. Sci., 25, 3653–3673, https://doi.org/10.5194/hess-25-3653-2021, 2021.

Prodhan, F.A., Zhang, J., Hasan, S.S., Pangali Sharma, T.P., Mohana, H.P.: A review of machine learning methods for drought hazard monitoring and forecasting: current research trends, challenges, and future research directions. Environ. Model. Software 149, 105327, https://doi.org/10.1016/j.envsoft.2022.105327, 2022.

Räsänen, T.A., Koponen, J., Lauri, H. et al.: Downstream Hydrological Impacts of Hydropower Development in the Upper Mekong Basin. Water Resour Manage 26, 3495–3513. https://doi.org/10.1007/s11269-012-0087-0, 2012.

Ren, J., Wang, W., Wei, J., Li, H., Li, X., Liu, G., Chen, Y., Ye, S.: Evolution and prediction of drought-flood abrupt alternation events in Huang-Huai-Hai River Basin, China. Sci. Total Environ. 869, https://doi.org/10.1016/j.scitotenv.2023.161707, 2023.

Sabo, J. L., Puhi, A., Holtgrieve, G. W., Elliott, V., Arias, M. E., Ngor, B. P., Räsänen, T. A., Nam, S.: Designing river flows to improve food security futures in the lower Mekong Basin. Science 358 (6368). https://doi.org/10.1126/science.aao1053, 2017.

Schmitt, R.J.P., Bizzi, S., Castelletti, A. et al.: Improved trade-offs of hydropower and sand connectivity by strategic dam planning in the Mekong. Nat Sustain 1, 96–104, https://doi.org/10.1038/s41893-018-0022-3, 2018.

Shan, L., Zhang, L., Song, J., Zhang, Y., She, D., Xia, J., 2018. Characteristics of dry-wet abrupt alternation events in the middle and lower reaches of the Yangtze River Basin and the relationship with ENSO. Acta Geographica Sinica, 73(1): 25-40 (in Chinese), https://doi.org/10.11821/dlxb201801003, 2018.

Shi, W., Huang, S., Liu, D., Huang, Q., Han, Z., Leng, G., Wang, H., Hao, L., Li, P., Wei, X.:

Drought-flood abrupt alternation dynamics and their potential driving forces in a changing environment. J. Hydrol. 597, 126179, https://doi.org/10.1016/j.jhydrol.2021.126179, 2021.

Sridhar, V., Kang, H., Ali, S.A.: Human-Induced Alterations to Land Use and Climate and Their Responses for Hydrology and Water Management in the Mekong River Basin. Water, 11, 1307, https://doi.org/10.3390/w11061307, 2019.

Song, X., Lei, X., Ma, R., Hou, J., Liu, W.: Spatiotemporal variation and multivariate controls of short-cycle drought–flood abrupt alteration: A case in the Qinling-Daba Mountains of China. International Journal of Climatology, 43(10), 4756–4769, https://doi.org/10.1002/joc.8115, 2023.

Sun, P., Zou, Y., Yao, R., Ma, Z., Bian, Y., Ge, C., Lv, Y.: Compound and successive events of extreme precipitation and extreme runoffunder heatwaves based on CMIP6 models. Science of the Total Environment, 878, 162980, https://doi.org/10.1016/j.scitotenv.2023.16298, 2023.

Tellman, B., Sullivan, J.A., Kuhn, C. et al.: Satellite imaging reveals increased proportion of population exposed to floods. Nature 596, 80–86, https://doi.org/10.1038/s41586-021-03695-w, 2021.

Tennant, D. L.: Instream flow regimens for fish, wildlife, recreation and related environmental resources. FISHERIES, 1(4), 6–10, https://doi.org/10.1577/1548-8446(1976)001<0006:IFRFFW>2.0.CO;2 1976.

Thompson, J., Green, A., & Kingston, D: Potential evapotranspiration-related uncertainty in climate change impacts on river flow: An assessment for the Mekong River basin. Journal of Hydrology, 510, 259–279. https://doi.org/10.1016/j.jhydrol.2013.12.010, 2014.

Tian, F., Liu, H., Hou, S., Li, K., Lu, H., Ni, G., Mu, X., Baiyinbaoligao: Drought characteristics of the Lancang-Mekong Basin and the role of reservoir regulation on streamflow. The international journal of hydropower&dams, 5, 81-89, http://www.thuwater.org/admin/tp/Report-on-Lancang-Mekong-Drought-and-Reservoir-Regulation.pdf (last access: March 2025), 2020.

Tian, F., Hu, H., Lei, Z., and Sivapalan, M.: Extension of the Representative Elementary Watershed approach for cold regions via explicit treatment of energy related processes, Hydrol. Earth Syst. Sci., 10, 619–644, https://doi.org/10.5194/hess-10-619-2006, 2006.

Tian, F., Li, H., Sivapalan, M.: Model diagnostic analysis of seasonal switching of runoff generation mechanisms in the Blue River basin, Oklahoma. J. Hydrol. 418 (419), 136–149, https://doi.org/10.1016/j.jhydrol.2010.03.011, 2012.

Van Pelt, S. C., Kabat, P., ter Maat, H. W., van den Hurk, B. J. J. M., and Weerts, A. H.: Discharge simulations performed with a hydrological model using bias corrected regional climate model input, Hydrol. Earth Syst. Sci., 13, 2387–2397, https://doi.org/10.5194/hess-13-2387-2009, 2009.

Wang, A., Miao, Y., Kong, X., & Wu, H: Future changes in global runoff and runoff coefficient from CMIP6 multi-model simulation under SSP1-2.6 and SSP5-8.5 scenarios. Earth's Future, 10(12), e2022EF002910. https://doi.org/10.1029/2022EF002910, 2022.

Wang, C., Leisz, S., Li, L., Shi, X., Mao, J., Zheng, Y., and Chen, A.: Historical and projected future runoff over the Mekong River basin, Earth Syst. Dynam., 15, 75–90, https://doi.org/10.5194/esd-15-75-2024, 2024.

Wang, R., Li, X., Zhang, Q., Cheng, J., Li, J., Zhang, D., Liu, Y.: Projection of drought-flood abrupt alternation in a humid subtropical region under changing climate. J. Hydrol. 624, 129875, https://doi.org/10.1016/j.jhydrol.2023.129875, 2023.

Wang, S., Zhang, L., She, D., Wang, G., Zhang, Q.: Future projections of flooding characteristics in the Lancang-Mekong River Basin under climate change. J. Hydrol. 602, https://doi.org/10.1016/j.jhydrol.2021.126778, 2021.

Wang, W., Li, H. Y., Leung, L. R., Yigzaw, W., Zhao, J., Lu, H., Deng, Z., Demisie, Y., Blöschl, G.: Nonlinear filtering effects of reservoirs on flood frequency curves at the regional scale, Water Resour. Res., 53, 8277–8292, https://doi.org/10.1002/2017WR020871,2017, 2017a.

Wang, W., Lu, H., Leung, L. R., Li, H.-Y., Zhao, J., Tian, F., Yang, K., Sothea, K.: Dam construction in Lancang-Mekong River Basin could mitigate future flood risk from warming-induced intensified rainfall. Geophysical Research Letters, 44, 10,378–10,386, https://doi.org/10.1002/2017GL075037, 2017b.

Wu, Z., Li, J., He, J., Jiang, Z.: Large-scale atmospheric singularities and summer long-cycle droughts–floods abrupt alternation in the middle and lower reaches of the Yangtze River. Chinese Science Bulletin, 51(16), 2027–2034, https://doi.org/10.1007/s11434-006-2060-x, 2006.

Williams, J. M.: The hydropower myth. Environ. Sci. Pollut. R, https://doi.org/10.1007/s11356-019-04657-6, 2019.

Xiong, J., Yang, Y.: Climate Change and Hydrological Extremes. Curr Clim Change Rep 11, 1, https://doi.org/10.1007/s40641-024-00198-4, 2025.

Yang, P., Zhang, S., Xia, J., Zhan, C., Cai, W., Wang, W., Luo, X., Chen, N., Li, J.: Analysis of drought and flood alternation and its driving factors in the Yangtze River Basin under climate change. J. ATMOS. RES. 270, 106087, https://doi.org/10.1016/j.atmosres.2022.106087, 2022.

Yang, Y., Weng, B., Bi, W., Xu, T., Yan, D., Ma, J.: Climate Change Impacts on Drought-Flood Abrupt Alternation and Water Quality in the Hetao Area, China. Water, 11, 652, https://doi.org/10.3390/w11040652, 2019.

Yuan, X., Wang, J.H., He, D.M., Lu, Y., Sun, J.R., Li, Y., Guo, Z.P., Zhang, K.Y., Li, F.: Influence of cascade reservoir operation in the upper Mekong River on the general hydrological regime: a combined data-driven modeling approach. J. Environ. Manag. 324, 116339, https://doi.org/10.1016/j.jenvman.2022.116339, 2022.

Yun, X.B., Tang, Q.H., Wang, J., Liu, X.C., Zhang, Y.Q., Lu, H., Wang, Y.L., Zhang, L., Chen, D.L.: Impacts of climate change and reservoir operation on streamflow and flood characteristics in the Lancang-Mekong River Basin. J. Hydrol. 590, 125472, https://doi.org/10.1016/j.jhydrol.2020.125472, 2020.

Yun, X., Tang, Q., Li, J., Lu, H., Zhang, L., Chen, D.: Can reservoir regulation mitigate future climate change induced hydrological extremes in the Lancang-Mekong River Basin? Sci. Total Environ. 785, https://doi.org/10.1016/j.scitotenv.2021.147322, 2021a.

Yun, X., Tang, Q., Sun, S., Wang, J.: Reducing climate change induced flood at the cost of hydropower in the Lancang-Mekong River Basin. Geophysical Research Letters, 48, e2021GL094243, https://doi.org/10.1029/2021GL094243, 2021b.

Zhang, D., Lin, J., Peng, Q., Wang, D., Yang, T., Sorooshian, S., Liu, X., Zhuang, J.: Modeling and simulating of reservoir operation using the artificial neural network, support vector regression, deep learning algorithm. J. Hydrol. 565, 720–736, https://doi.org/10.1016/j.jhydrol.2018.08.050, 2018.

Zhang, K., Morovati, K., Tian, F., Yu, L., Liu, B., Olivares, M.A.: Regional contributions of climate change and human activities to altered flow of the Lancang-Mekong river. J. Hydrol.: Reg. Stud. 50, 101535, https://doi.org/10.1016/j.ejrh.2023.101535, 2023.

Zhang, S., Zhang, J., Min, J., Zhang, Z., Zhuang, J., Lin, J.: Drought–flood abrupt alternation based on runoff in the Huaihe River Basin during rainy season. Journal of Lake Sciences, 24(5), 679–686 (in Chinese), https://doi.org/10.18307/2012.0506, 2012.

Zhang, Z.Z., Yuan, Y.J., Shen, D.F., Fan, H.: Identification of drought-flood Abrupt alternation in tobacco growth period in Xingren county under climate change in China. Appl. Ecol. Environ. Res. 17, 12259–12269, https://doi.org/10.15666/aeer/1705_1225912269, 2019.

Zhao, D., Deng, S., Zhang, J.: Spatiotemporal characteristics of dry-wet abrupt alternation events in China during 1960–2018. International Journal of Climatology, 42(16), 9612–9625, https://doi.org/10.1002/joc.7850, 2022.